Age and BMI have different effects on subcutaneous, visceral, liver, bone marrow, and muscle adiposity, as measured by CT and MRI

Wang, L.; Liu, Y.D.; Li, K.; Zhang, W.S.; Yuan, Y.; Ma, K.K.; ... ; Vlug, A.G.

Received: 8 December 2023 | Revised: 15 March 2024 | Accepted: 19 March 2024

DOI: 10.1002/oby.24040

ORIGINAL ARTICLE

Obesity Biology and Integrated Physiology

Obesity A Research Journal | THE OBESITY SOCIETY | WILEY

Age and BMI have different effects on subcutaneous, visceral, liver, bone marrow, and muscle adiposity, as measured by CT and MRI

Ling Wang[1,2] | Yandong Liu[1] | Kai Li[1] | Wenshuang Zhang[1] | Yi Yuan[1] | Kangkang Ma[1] | Fengyun Zhou[1] | Zitong Cheng[1] | Jian Geng[1] | Yongbin Su[1] | Zhe Guo[1] | Glen M. Blake[3] | Xiaoguang Cheng[1] | Yajun Liu[2,4] | Klaus Engelke[5,6] | Annegreet G. Vlug[7]

[1]Department of Radiology, Beijing Jishuitan Hospital, Capital Medical University, National Center for Orthopaedics, Beijing, China

[2]JST Sarcopenia Research Centre, Beijing Research Institute of Traumatology and Orthopaedics, Beijing Jishuitan Hospital, Capital Medical University, National Center for Orthopaedics, Beijing, China

[3]School of Biomedical Engineering & Imaging Sciences, King's College London, St Thomas' Hospital, London, UK

[4]Department of Spine Surgery, Beijing Jishuitan Hospital, Capital Medical University, National Center for Orthopaedics, Beijing, China

[5]Institute of Medical Physics, University Erlangen–Nuremberg, Nuremberg, Germany

[6]Department of Medicine 3 - Rheumatology and Immunology, FAU University of Erlangen–Nuremberg and University Hospital Erlangen, Erlangen, Germany

[7]Center for Bone Quality, Department of Internal Medicine, Leiden University Medical Center, Leiden, the Netherlands

Correspondence
Xiaoguang Cheng
Email: xiao65@263.net

Yajun Liu
Email: drliuyajun@163.com

Funding information
Beijing Municipal Public Welfare Development and Reform Pilot Project for Medical Research Institutes, Grant/Award Numbers: JYY2023-11, JYY2023-8; Beijing Municipal Health Commission, Grant/Award Number: BJRITO-RDP-2024; National Natural Science Foundation of China, Grant/Award Numbers: 82371957, 82371956; Beijing Hospitals Authority Clinical Medicine Development of Special Funding Support, Grant/Award Number: ZYLX202107; Beijing Hospitals Authority Youth Programme, Grant/Award Number: QML20200402; Beijing Hospitals Authority's Ascent Plan, Grant/Award Number: DFL20220401

Abstract

Objective: We analyzed quantitative computed tomography (CT) and chemical shift–encoded magnetic resonance imaging (MRI) data from a Chinese cohort to investigate the effects of BMI and aging on different adipose tissue (AT) depots.

Methods: In 400 healthy, community-dwelling individuals aged 22 to 83 years, we used MRI to quantify proton density fat fraction (PDFF) of the lumbar spine (L2–L4) bone marrow AT (BMAT), the psoas major and erector spinae (ES) muscles, and the liver. Abdominal total AT, visceral AT (VAT), and subcutaneous AT (SAT) areas were measured at the L2-L3 level using quantitative CT. Partial correlation analysis was used to evaluate the relationship of each AT variable with age and BMI. Multiple linear regression analysis was performed in which each AT variable was evaluated in turn as a function of age and the other five independent AT measurements.

Results: Of the 168 men, 29% had normal BMI (<24.0 kg/m^2), 47% had overweight (24.0–27.9 kg/m^2), and 24% had obesity (≥ 28.0 kg/m^2). In the 232 women, the percentages were 46%, 32%, and 22%, respectively. Strong or very strong correlations with BMI were found for total AT, VAT, and SAT in both sexes. BMAT and ES PDFF was strongly correlated with age in women and moderately correlated in men. In both sexes, BMAT PDFF correlated only with age and not with any of the other AT depots. Psoas PDFF correlated only with ES PDFF and not with age or the other AT

depots. Liver PDFF correlated with BMI and VAT and weakly with SAT in men. VAT and SAT correlated with age and each other in both sexes.

Conclusions: Age and BMI are both associated with adiposity, but their effects differ depending on the type of AT.

INTRODUCTION

Populations are aging, and obesity rates are rising in both developed and developing countries [1]. Obesity is defined by the World Health Organization (WHO) as abnormal or excessive fat accumulation that presents a risk to health, which is commonly translated in clinical practice into a classification dependent on body mass index (BMI) with different cutoffs depending on ethnic background [2]. Aging is also associated with an increase in fat mass, and both aging and increased BMI are associated with an increased prevalence of insulin resistance, diabetes, metabolic dysfunction, cardiovascular disease, and cancer [3].

Adipose tissue (AT), primarily composed of adipocytes or fat cells containing lipid droplets, is distributed throughout the body in several depots such as subcutaneous and visceral adipose tissue (SAT, VAT). However, adipocytes and liquid droplets also accumulate in non-adipose tissues, including muscle, bone marrow (BM), and liver [4]. This excess storage of adipocytes and lipids in different organs contributes to the pathogenesis of many diseases [5]. Several studies have shown that the inflammatory profile, adipokine expression, and type of adipocyte differ among the fat depots [6], which could also alter the effect on disease development [7].

Although the common definition of obesity is based on BMI, the risk of disease seems to be more dependent on AT distribution and body composition than BMI [8]. Body composition, or the distinction between fat mass and lean mass, is often determined using dual-energy x-ray absorptiometry or bioelectrical impedance analysis. However, more advanced imaging methods such as quantitative magnetic resonance imaging (MRI) allow for further distinction between SAT and VAT and measurement of other AT depots such as muscle and bone marrow AT (BMAT) [9].

Several studies have investigated the relationship between either age or BMI and mostly one or two AT depots [3, 10–12], but no studies to date, to our knowledge, have studied the relationship between both age and BMI in one population for multiple AT depots using state-of-the-art imaging techniques. Therefore, the aim of this study was to use state-of-the-art three-dimensional quantitative imaging technology, including computed tomography (CT) and proton density fat fraction (PDFF) MRI, to better characterize the comparative effects of BMI and aging on different AT depots and their interactions in cross-sectional CT and MRI through the abdomen. A large cohort of community-dwelling Chinese men and women with ages ranging over six decades who were already enrolled in a study of age-related degeneration of the spine [13] was used for the purpose of this study.

Study Importance

What is already known?

- Throughout the world, populations are aging, and obesity rates are rising, causing significant changes in body composition.
- The increase in fat mass affects energy metabolism and is a major factor in the development of insulin resistance, diabetes, metabolic dysfunction, cardiovascular disease, and cancer.

What does this study add?

- This is the first study, to our knowledge, to measure multiple adipose tissue (AT) depots in the same individuals across a wide range of ages and BMI values, and it gives new insights into the relative effects of aging and obesity on different types of fat depots.
- We show, for the first time, to our knowledge, that age and BMI are independently associated with adiposity and that, depending on anatomical location, the magnitude of the effect differs for aging and obesity.
- Visceral and subcutaneous AT areas are more strongly correlated with obesity, whereas bone marrow and muscle proton density fat fraction is more strongly correlated with age.

How might these results change the direction of research or the focus of clinical practice?

- A better understanding of the relationship between the different fat depots with aging and obesity might facilitate the development of new pharmacological approaches that may ultimately delay or reverse the negative consequences of adiposity-related dysfunction such as diabetes, cardiovascular disease, hepatosteatosis, osteoporosis, and sarcopenia.

METHODS

Study participants

A total of 400 adults without serious health problems (232 women, 168 men; age range, 22–83 years; mean age, 52.7 years), a subset of previously enrolled participants of a longitudinal study, were included

in the current study. The earlier study commenced in June 2014 and was conducted in the Department of Spine Surgery at Beijing Jishuitan Hospital (Beijing, China). Its aim was the investigation of the development of spinal degenerative disease and its related risk factors [14]. All participants in the substudy were recruited from communities close to the hospital and volunteered to also participate in the study presented here. As part of the earlier study, routine lumbar spine quantitative CT (QCT) scans had been performed, which were reanalyzed for the present study. In addition, the subcohort of 400 adults had also undergone an additional chemical shift–encoded (CSE)-MRI scan [13, 14].

The inclusion criteria were independent community-dwelling adults aged 20 years or older who were able to give informed consent. Pregnant women, individuals with metal implants in the thoracicolumbar spine, and people intolerant of MRI examinations were excluded. The exclusion criteria also included stroke, neurologic disorders, metabolic diseases (not including diabetes), rheumatic diseases, severe spinal degenerative disease, spine tumors, heart failure, severe cardiovascular complications, severe chronic obstructive pulmonary disease, coagulation disorders, and other diseases that limited function. Furthermore, the subset did not include individuals with cachexia or anorexia nervosa. The study was approved by the institutional review board of Beijing Jishuitan Hospital (no. 201210-08), and written informed consent was obtained from all study participants.

QCT scan protocol and measurements of AT

QCT scans of the lumbar spine (L1–L5) were performed using a Toshiba CT scanner (Aquilion PRIME ESX-302A; Toshiba Medical Systems Corp., Otawara, Japan) with a Mindways calibration phantom (Mindways Software Inc., Austin, Texas) placed beneath the participants. Scan parameters were 120 kilovolts (peak) (kV[p]); 187 mAs (milliampere-seconds); 40-cm collimation; 120-cm table height; scan field of view (FOV) of 500 mm; and section thickness of 1 mm. Reconstruction parameters were a medium reconstruction kernel (FC08), a reconstructed section thickness and a reconstruction interval of 1 mm each, and a 400-mm reconstruction FOV.

QCT measurements of total AT (TAT) and VAT area were performed at the L2-L3 level using the Mindways QCT-Pro Tissue Composition Module (Mindways Software; Figure 1A). The L2-L3 section typically intersects the umbilicus. This location is consistent with other CT protocols for abdominal AT assessments. SAT, defined as the area of AT between the skin and the rectus muscles of the abdomen, the external oblique muscles, i.e., the broadest muscle of the back, and the erector muscles of the spine, was measured as SAT = TAT − VAT. VAT was defined as the entire intra-abdominal AT area within the abdominal cavity of the rectus, external oblique, lumbar quadrate, and psoas (PS) muscles. All of the measurements were carried out by an experienced radiologist (Zhe Guo) trained in QCT techniques.

The lateral CT scout view image of T7 to L4 was used to assess vertebral fracture according to Genant's semiquantitative method, as previously described [15]; each vertebral body was graded as normal (grade 0, normal and <20% height reduction), mild (grade 1, 20%–25% height reduction and 10%–20% in area), moderate (grade 2, 25%–40% height reduction and 20%–40% in area), or severe (grade 3, >40% in height and area) fracture. The reading was done by an expert musculoskeletal radiologist (Xiaoguang Cheng) with more than 30 years of experience in vertebral fracture assessment.

CSE-MRI protocol and MRI measurements of PDFF

On the same day as the QCT examination, the participants underwent an mDIXON-Quant study on a 3-T MR scanner (Ingenia, Philips Healthcare, Best, the Netherlands) with a 32-channel Torso body coil (Figure 1B). The mDIXON-Quant sequence is a 6-point Dixon sequence. The scan parameters were as follows: repetition time (TR) = 6.2 ms; first echo time (TE1) = 0.95 ms; 6 echoes with TE shift (ΔTE) = 0.8 ms; FOV = 360 × 330 × 120 mm^3; flip angle (FA) = 3°; voxel size = 2.5 × 2.5 × 3.0 mm^3; sensitivity encoding = 2; and number of signal averages = 2.

The CSE-MRI data were processed with the ISP software (version 7; Philips Healthcare). PDFF maps were generated for the measurement of tissue fat fraction. Measurements included BMAT PDFF, liver PDFF, and PDFF of the PS and erector spinae (ES) muscles. BMAT PDFF was measured by manually drawing regions of interest (ROIs) encompassing the largest region of cancellous bone in the vertebral bodies on the central L2-L3-L4 axial single section images (Figure 1C). PDFF of PS and ES muscles was measured on the same central L2–L4 axial images as BMAT PDFF (Figure 1C).

Liver PDFF was measured by placing three ROIs, each with an area of 300 mm^2, in the peripheral areas of the left lobe, the right anterior lobe, and the right posterior lobe, respectively, in the section in which the right branch of the portal vein enters the liver (Figure 1D). The ROIs were selected to avoid major blood vessels and bile ducts, intrahepatic calcification, liver cysts, artifacts caused by the ribs, and gas in the lung or gastrointestinal tract visible on MRI. The average of the ROIs was used for the MRI measurements of BMAT, paraspinal muscle, and liver PDFF. All of the measurements were carried out by an experienced radiologist (Zhe Guo) trained in MRI techniques. The precision results of the CSE-MRI measurements have been reported in previous studies [13, 16].

Statistical analysis

Statistics Kingdom statistical software (Melbourne, Australia) was used for data analysis. The demographic characteristics of the study participants were expressed as mean and standard deviation, separately for men and women and for different categories of age and BMI. BMI was calculated as weight in kilograms divided by height in meters squared. Based on the Chinese population cutoffs, BMI results were classified as normal (BMI < 24), overweight (24–27.9), or obesity (≥28). Using the thresholds proposed by Xu et al., visceral obesity was defined as a VAT area at the L2-L3 level of >142 cm^2 in men

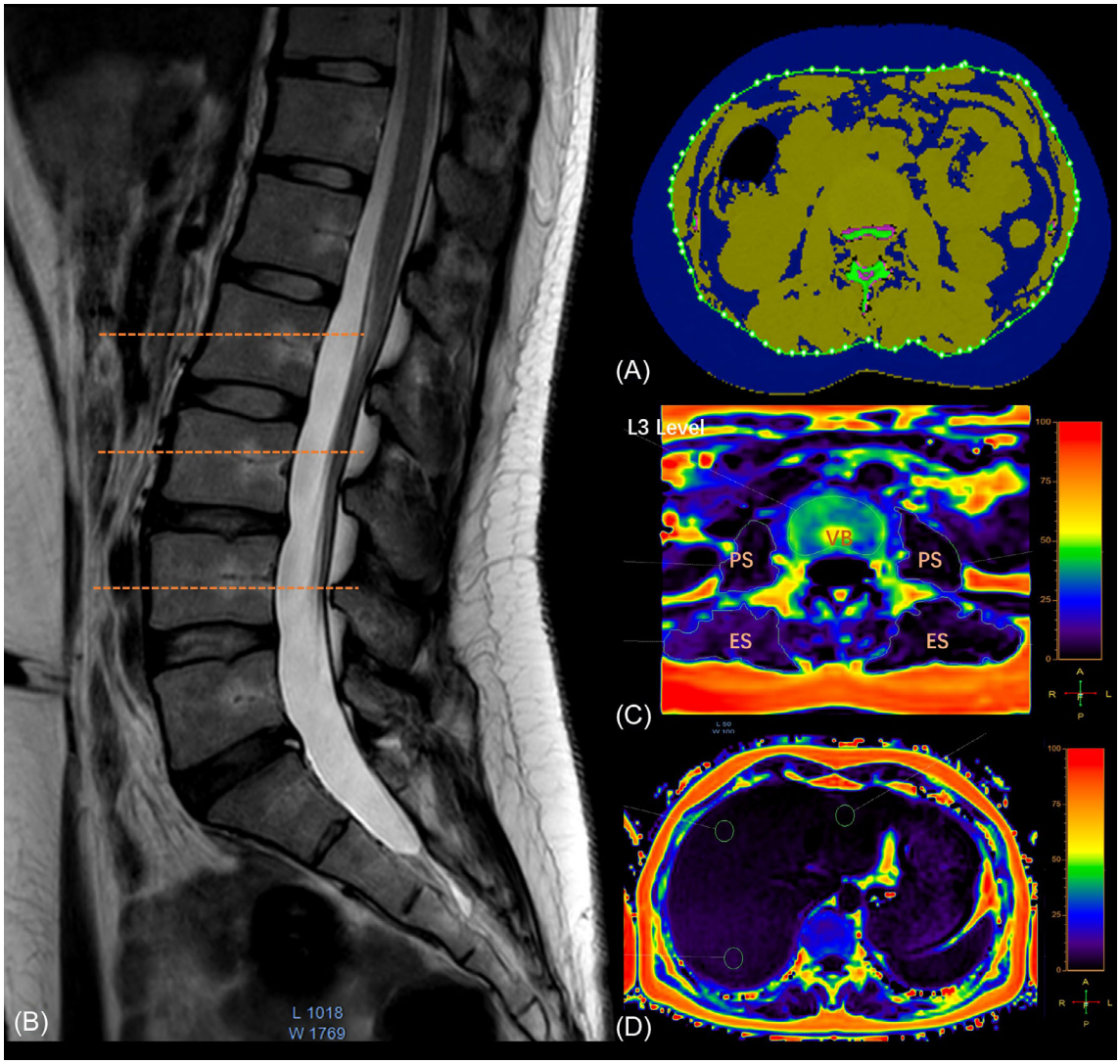

FIGURE 1 (A) Computed tomography image of the plane through L2 and L3. Green dots show the region of interest (ROI) demarcating visceral and subcutaneous adipose tissue (VAT, SAT). (B) MRI of the lower thoracic spine, lumbar spine, and sacrum. Horizontal dashed lines through L2, L3, and L4 show the planes for bone marrow adipose tissue (BMAT) proton density fat fraction (PDFF) measurements, and the average of the three vertebrae was chosen for the BMAT PDFF. (C) MRI of the plane through L3 showing the ROIs delineating the vertebral body (VB) for the measurement of BMAT PDFF, the psoas muscles (PS), and the erector spinae muscles (ES). (D) MRI through the liver showing the three ROIs in the left lobe, right anterior lobe, and right posterior lobe used to measure liver PDFF. [Color figure can be viewed at wileyonlinelibrary.com]

and >115 cm^2 in women [17]. Normal liver fat content was defined as PDFF <5.0%, mild steatosis as PDFF between 5.0% and 14.9%, moderate steatosis as PDFF between 15.0% and 24.9%, and severe steatosis as PDFF ≥ 25% [13]. Sexual dimorphism was expressed as the mean difference between men and women expressed as a percentage of female values.

Scatterplots were drawn of BMI against age for men and women, respectively, and the relationships were evaluated using the Pearson correlation coefficient. Similar scatterplots were drawn of TAT, VAT, SAT, and PS muscle, ES muscle, liver, and BMAT PDFF against age and BMI for men and women, and the partial correlation coefficients were evaluated. A square of a partial correlation coefficient of $r^2 \geq 0.640$ was considered very strong, $r^2 = 0.360$ to 0.639 was considered strong, $r^2 = 0.160$ to 0.359 was considered moderate, $r^2 = 0.040$ to 0.159 was considered weak, and $r^2 < 0.040$ was considered very weak. Multiple linear regression (MLR) analysis was used to investigate the dependence of each AT measurement on BMI and age. In the absence of any appreciable correlation between BMI and age in either sex, the squares of the standardized coefficients were interpreted as the fraction of the total variance of each AT variable accounted for by BMI and age, respectively. A second MLR analysis was performed in which each PDFF or area variable was evaluated as a linear function of age and the other five independent AT measurements. TAT was excluded from this latter analysis because it is

calculated as the sum of VAT and SAT and is not an independent measurement. Because there were significant correlations between some pairs of independent variables in the MLR analysis, the results were assessed using the squares of the partial correlation coefficients and their p values. A p value < 0.05 was considered to be statistically significant.

RESULTS

Participant characteristics

Table 1 lists the demographic characteristics of the 400 individuals who participated in the study. Of the 168 men, 29% had normal BMI (<24.0), 47% had overweight (24.0–27.9), and 24% had obesity (≥28.0). For the 232 women, the percentages were 46%, 32%, and 22%, respectively. Tables S1 and S2 show participant characteristics broken down by BMI (Table S1) and age (Table S2). A total of 74% of the men had a VAT measurement greater than the male upper limit of normal of 142 cm^2 compared with 59% of women with a VAT greater than the female upper limit of 115 cm^2. When assessed for liver PDFF, 50% of men had normal liver fat (PDFF < 5.0%), whereas 41% had mild (5.0%–14.9%), 8% had moderate (15.0%–24.9%), and 1% had severe steatosis (≥ 25%). For women, these percentages were 65%, 30%, 5%, and 0%, respectively. Table S3 shows results of the sexual dimorphism analysis expressed as the percentage difference between mean male and female measurements normalized to female values. In general, men had lower muscle adiposity (−18% and −34%; $p < 0.001$) but higher liver fat (23%; $p < 0.01$) compared with women. There was no significant difference in L2–L4 BM fat between men and women generally, but women had lower BMAT in the young age group (−23%; $p < 0.001$) and higher BMAT in the old age group (9%; $p < 0.001$) compared with men.

Correlation of AT with aging and BMI

In men, BMI and age were not significantly correlated ($r^2 = 0.002$; $p = 0.59$; Figure 2). In women, there was a weak correlation ($r^2 = 0.083$; $p < 0.001$). On average, women aged 50 years and older had a significantly higher BMI than those aged less than 50 years (25.8 vs. 23.6; $p < 0.001$), most likely due to menopausal hormonal changes.

Figures S1 through S7 show the correlations of the TAT, VAT, and SAT areas and PS muscle, ES muscle, L2–L4 BMAT, and liver PDFF values with age and BMI. In each plot, the r^2 value and its associated p value relate to the partial correlation analysis with age and BMI as the independent variables. Strong or very strong correlations with BMI were found for TAT, VAT, and SAT areas in both sexes. BMAT PDFF and ES PDFF were both strongly correlated with age in women and moderately correlated with age in men. Most other correlations were weak or very weak (Table S4).

Figure 3 presents bar charts for men and women showing the squares of the standardized coefficients for BMI and age found in the MLR analysis. The error bars are the 95% confidence intervals (CI). The p values are the same as those in the online Supporting Information figures. Given the weak or very weak correlations between BMI and age, the standardized coefficients represent the fraction of

TABLE 1 Demographic characteristics of the 400 participants.

	Men ($n = 168$)	Women ($n = 232$)	p value
Age (22–83 y)	51.5 ± 15.0	53.5 ± 15.8	NS
Height (cm)	170.6 ± 6.2	158.3 ± 6.1	<0.001
Weight (kg)	76.3 ± 12.6	62.6 ± 9.3	<0.001
BMI (kg/m^2)	26.1 ± 3.6	25.0 ± 3.8	<0.01
Waist circumference (cm)	91.4 ± 9.3	83.5 ± 9.8	<0.001
Hip circumference (cm)	100.0 ± 7.0	97.6 ± 8.7	<0.01
Waist-hip ratio	0.913 ± 0.060	0.856 ± 0.074	<0.001
Average vBMD (mg/cm^3)	134.8 ± 41.4	125.5 ± 55.8	NS
Asymptomatic vertebral fracture prevalence, n (%)	30 (19.1)	30 (13.9)	NS
Mild vertebral fracture, n (%)	24 (15.3)	20 (9.3)	NA
BMAT PDFF (%)	42.8 ± 8.5	43.8 ± 11.5	NS
SAT (L2–L3) area (cm^2)	120.0 ± 60.9	149.3 ± 64.9	<0.001
VAT (L2–L3) area (cm^2)	199.1 ± 78.9	141.8 ± 65.9	<0.001
PS PDFF (%)	5.6 ± 3.2	6.8 ± 4.1	<0.001
ES PDFF (%)	6.7 ± 4.8	10.0 ± 6.6	<0.001
Liver PDFF (%)	7.1 ± 5.5	5.7 ± 4.2	<0.01

Abbreviations: BMAT, bone marrow adipose tissue; ES, erector spinae; NS, not statistically significant; PDFF, proton density fat fraction; PS, psoas muscle; SAT, subcutaneous adipose tissue; VAT, visceral adipose tissue; vBMD, volumetric bone mineral density.

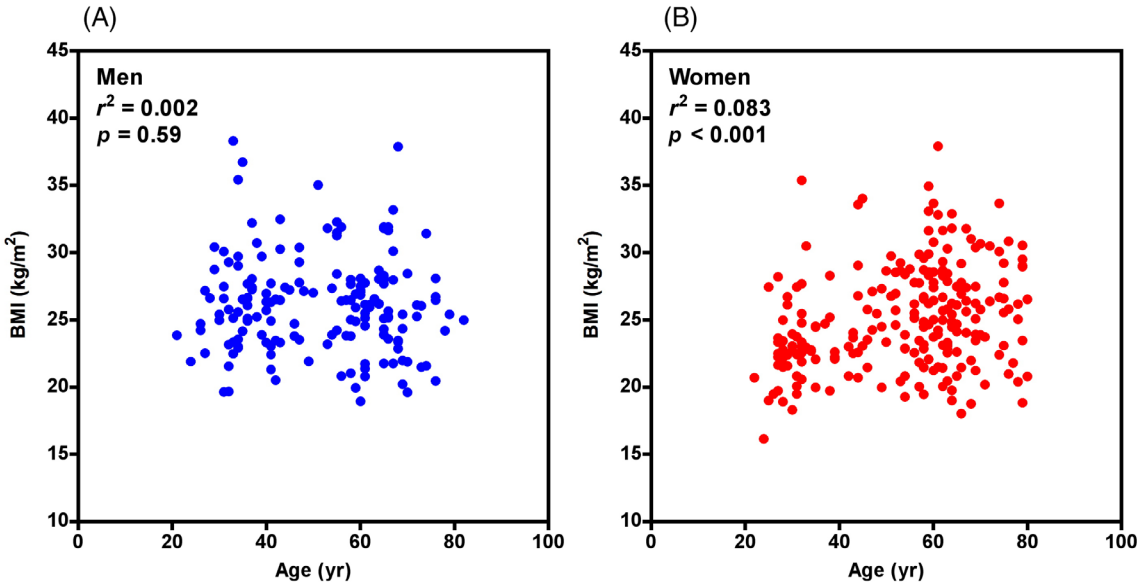

FIGURE 2 Scatterplots of BMI versus age in (A) men ($n = 168$) and (B) women ($n = 232$). r^2 is the square of Pearson correlation coefficient. [Color figure can be viewed at wileyonlinelibrary.com]

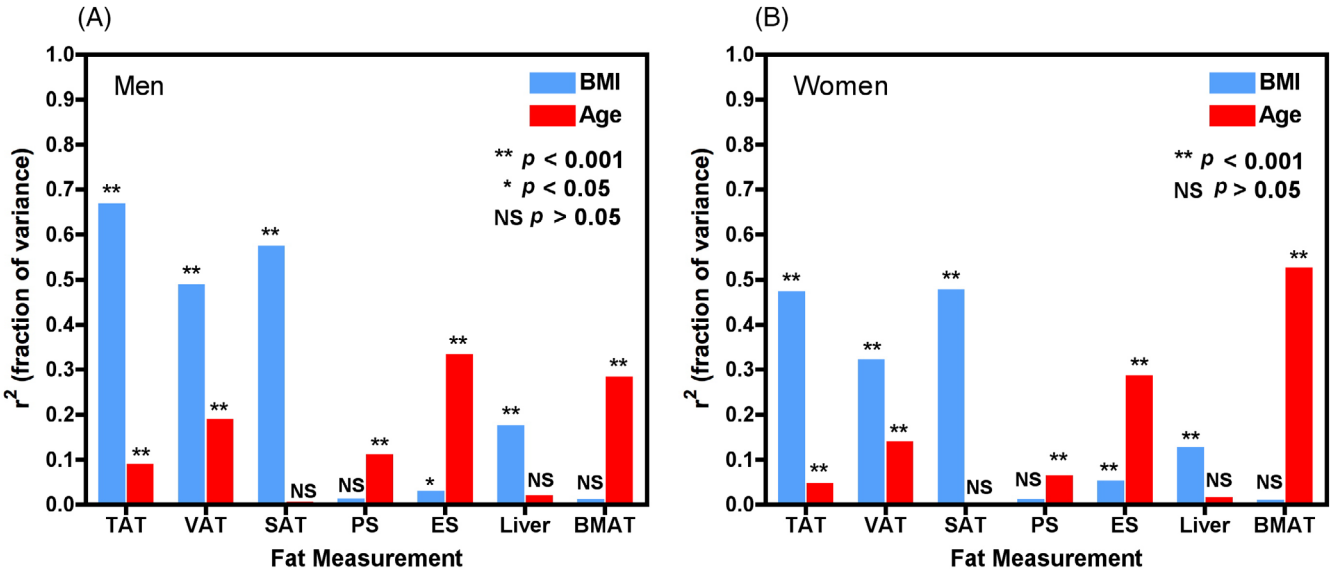

FIGURE 3 Bar charts comparing the squares of the standardized coefficients for BMI and age derived by multiple linear regression (MLR) analysis of the MRI proton density fat fraction (PDFF) and computed tomography area measurements at seven different sites of adipose tissue: (A) men and (B) women. BMAT, bone marrow adipose tissue PDFF; ES, erector spinae muscle PDFF; Liver, liver PDFF; NS, not statistically significant; PS, psoas muscle PDFF; SAT, subcutaneous adipose tissue area; TAT, total adipose tissue area (TAT = VAT + SAT); VAT, visceral adipose tissue area. Error bars show the 95% CI. In the absence of any significant collinearity between the two independent variables (Figure 2), the squares of the standardized coefficients plotted in the figure represent the fraction of the total variance of each of the adipose tissue measurements attributable to BMI and age, respectively. [Color figure can be viewed at wileyonlinelibrary.com]

the total variance of the PDFF and area AT measurements accounted for by BMI and age, respectively, allowing a comparison of the relative importance of these two factors.

Tables 2 and 3 present the results of the further MLR analysis, in which each AT variable was evaluated as a function of age and each of the other five independent AT variables. For the reasons explained earlier, TAT was not included in this analysis. Because of issues with significant multicollinearity between some of the variables, the results are shown as the squares of the partial correlation coefficients with age and each of the other five AT measurements. As with Figure 3, the results for men and women were similar. Notably, in both sexes, BMAT PDFF correlated only with age. PS PDFF correlated only with

TABLE 2 Men ($n = 168$): results of partial correlation analysis between each AT variable and age and the five independent fat variables.

AT variable	Age	BMAT PDFF	ES PDFF	PS PDFF	Liver PDFF	SAT area	VAT area	Adjusted r^2
BMAT PDFF	$r^2 = 0.280$ $p < 0.001$	-	NS	NS	NS	NS	NS	0.280
ES PDFF	$r^2 = 0.219$ $p < 0.001$	NS	-	$r^2 = 0.248$ $p < 0.001$	NS	NS	$r^2 = 0.046$ $p < 0.01$	0.510
PS PDFF	NS	NS	$r^2 = 0.333$ $p < 0.001$	-	NS	NS	NS	0.333
Liver PDFF	$r^2 = 0.104$ $p < 0.001$	NS	NS	NS	-	$r^2 = 0.043$ $p < 0.05$	$r^2 = 0.163$ $p < 0.001$	0.333
SAT (L2–L3) area	$r^2 = 0.063$ $p < 0.01$	NS	NS	NS	$r^2 = 0.038$ $p < 0.05$	-	$r^2 = 0.358$ $p < 0.001$	0.381
VAT (L2–L3) area	$r^2 = 0.241$ $p < 0.001$	NS	NS	$r^2 = 0.047$ $p < 0.001$	$r^2 = 0.108$ $p < 0.001$	$r^2 = 0.298$ $p < 0.001$	-	0.536

Note: r^2 is the square of the partial correlation coefficient. Adjusted r^2: fraction of total variance explained by age and the five independent PDFF/area variables.
Abbreviations: AT, adipose tissue; BMAT, bone marrow AT; ES, erector spinae; NS, not statistically significant; PDFF, proton density fat fraction; PS, psoas muscle; SAT, subcutaneous adipose tissue; VAT, visceral adipose tissue.

TABLE 3 Women ($n = 232$): results of partial correlation analysis between each AT variable and age and the five independent fat variables.

AT variable	Age	BMAT PDFF	ES PDFF	PS PDFF	Liver PDFF	SAT area	VAT area	Adjusted r^2
BMAT PDFF	$r^2 = 0.583$ $p < 0.001$	-	NS	NS	NS	NS	NS	0.583
ES PDFF	$r^2 = 0.281$ $p < 0.001$	NS	-	$r^2 = 0.093$ $p < 0.001$	NS	NS	$r^2 = 0.130$ $p < 0.001$	0.521
PS PDFF	NS	NS	$r^2 = 0.180$ $p < 0.001$	-	NS	NS	NS	0.180
Liver PDFF	NS	NS	NS	NS	-	NS	$r^2 = 0.201$ $p < 0.001$	0.201
SAT (L2–L3) area	$r^2 = 0.097$ $p < 0.001$	NS	NS	NS	NS	-	$r^2 = 0.557$ $p < 0.001$	0.480
VAT (L2–L3) area	$r^2 = 0.251$ $p < 0.001$	NS	$r^2 = 0.065$ $p < 0.01$	NS	$r^2 = 0.087$ $p < 0.001$	$r^2 = 0.406$ $p < 0.001$	-	0.672

Note: r^2 is the square of the partial correlation coefficient. Adjusted r^2: fraction of total variance explained by age and the five independent PDFF/area variables.
Abbreviations: AT, adipose tissue; BMAT, bone marrow AT; ES, erector spinae; NS, not statistically significant; PDFF, proton density fat fraction; PS, psoas muscle; SAT, subcutaneous adipose tissue; VAT, visceral adipose tissue.

ES PDFF and not with age or the other PDFF measurements. Liver PDFF correlated with age and VAT and weakly with SAT in men. VAT and SAT correlated with age and with each other in both sexes.

DISCUSSION

In this study of a large group of community-dwelling Chinese men and women with a broad age and BMI range, we showed, with advanced imaging methods, that aging and BMI affect the diverse AT depots in the abdominal region of the body differently; VAT and SAT were mostly associated with BMI, whereas BM and muscle AT were mostly associated with age. In addition, we showed that subcutaneous visceral and liver AT depots clustered in their response to age and BMI, whereas muscle and BMAT behave independently of other AT depots.

Body composition changes reflect increases in weight due to caloric excess. Many studies have shown that, initially, these calories are stored as lipids in the SAT without important disruptions in systemic energy metabolism [8, 18]. However, with increasing calorie

excess, an inflammatory response is induced in SAT, and lipids start to accumulate in the VAT and the liver, leading to further inflammation, insulin resistance, lipid toxicity, and hepatosteatosis and ultimately resulting in diabetes and cardiovascular disease [19–23].

BM fat, the AT present in BM, has been the subject of intense study over the past two decades due to its association with osteoporosis, skeletal metastases, and hematological diseases [24]. One of the most studied conditions in relationship to BM adiposity is anorexia nervosa, in which the paradoxical increase in BMAT coincides with vanishing subcutaneous and visceral fat due to severe caloric restriction [25]. On the contrary, the response of BMAT to obesity is less clear, and some studies have reported no change or some increase in BMAT [26] depending on the diabetic status.

Interestingly, the inflammatory response to obesity seems to differ among the different AT depots. Tencerova et al. [27] compared the expression of inflammatory, insulin-signaling, and adipogenic genes in mice in lean versus high-fat diet-induced obesity conditions and showed that, whereas there was a strong inflammatory response in VAT, this was not present in BMAT. In addition, a study by Attane et al. [28] showed that, whereas the lipid metabolism in white adipocytes present in SAT and VAT is focused on lipolysis, BMAT adipocytes show a cholesterol-oriented metabolism and are relatively deficient in lipolysis.

Aging also affects body composition, with an increase in fat mass and a decrease in lean and muscle mass, and is associated with increased inflammation and a higher prevalence of diabetes and cardiovascular diseases [19, 20]. Some researchers even consider obesity as "accelerated aging" due to the shared underlying inflammatory mechanisms [8, 29]. Nowadays, for many people, aging and obesity are both present, resulting in even higher risks of disease and premature death. Also, BM and muscle adiposity increase with aging and possibly negatively influence the integrity and function of the bone [30] and muscle tissue [10].

It is known that osteoporosis and vertebral fracture risk are associated with increased BM fat and that hip fracture risk is associated with increased muscle fat infiltration [23, 31–33]. A recent analysis of the Age Gene/Environment Susceptibility (AGES)-Reykjavik study concluded that increased amount of saturated lipids in BM were associated with increased vertebral fracture risk, whereas unsaturated lipids were associated with decreased vertebral fracture risk [34]. In our study, we could not differentiate the associations of the unsaturated and saturated lipids, which requires the use of MR spectroscopy.

Although SAT accounts for about 85% of all body fat in people [35], our study indicates that, in men, the abdominal SAT had no association with ectopic fats except for liver fat, and, in women, SAT is not associated with any ectopic fat. Previous studies have shown a stronger association between liver fat and obesity than with age [11, 36], and liver fat accumulation may also be due to age-related changes in subcutaneous fat. Accordingly, liver fat is generally reported to be more strongly associated with visceral adiposity [4]. Unlike other ectopic fat depots, BMAT is generally not related to obesity in humans [37]. Our observations also confirm this finding.

The PS muscle plays a key role in maintaining posture and core strength [38]; therefore, it might be considered a suitable biomarker of sarcopenia. However, our results showed that PS PDFF correlated only with ES PDFF and not with age or the other PDFF measurement, suggesting that PS muscle assessment may not be a good indicator of sarcopenia after all. In line with this, a recent study found that the PS muscle index has poor performance for predicting liver transplant waitlist mortality in patients with cirrhosis [39].

Hormones such as estrogen, insulin, cortisol, and many others profoundly influence adipocytes and regulate many processes related to energy metabolism. This is exemplified in the differences in body composition and energy metabolism between men and women, and, more specifically, between pre- and postmenopausal women. Also in our cohort, we did not find a relationship between age and BMI in men. However, in women, there was a clear increase in BMI with aging. Therefore, we have presented the results for men and women separately.

The present study has several limitations. Although we performed our study in a large cohort, the number of participants was restricted by the limited resources for these expensive and time-consuming imaging methods. Nonetheless, this is the first study, to our knowledge, to measure all of the AT depots present in the abdominal region across wide age and BMI ranges. Therefore, it represents a unique opportunity to compare the effects of aging and obesity. It is a limitation that only a very limited number of CT and MRI sections were used; therefore, a true volumetric analysis could not be performed.

Also, our cohort is limited to Chinese individuals; therefore, our results need to be confirmed in populations of different ethnicity. The cross-sectional design limits our analyses to associations; prospective studies will give more insight into the natural development of AT.

Furthermore, in this cohort with a large age range, a high BMI does not always reflect obesity. In particular, in younger men, BMI may be increased due to higher muscle mass, whereas, in old age in both sexes, BMI may be decreased by a loss in muscle mass. Unfortunately, dual-energy x-ray absorptiometry- or bioelectrical impedance analysis-based total adiposity measures were not available in this study, which impedes our understanding of how total adiposity impacts other organ fats with aging [40]. Finally, we did not measure gluteofemoral fat, which is an important contributor of AT distribution with aging in men and women.

CONCLUSION

In summary, in this study, we show, with advanced imaging methods in a large group of Chinese men and women, that both age and BMI are associated with adiposity in the abdominal region, but the magnitude of the differential effect for age versus BMI strongly depends on the type of AT and its anatomical location. The mechanisms of age- and obesity-related fat accumulation and redistribution are interconnected and modulate each other, thereby constituting an integrated network. A better understanding of the relationship between the

different fat depots with aging and BMI might facilitate targeting specific pharmacological approaches that may ultimately delay or reverse the negative consequences of adiposity-related dysfunction such as diabetes, cardiovascular disease, hepatosteatosis, osteoporosis, and sarcopenia.O

AUTHOR CONTRIBUTIONS

Study concept and design: Ling Wang, Annegreet G. Vlug, Yajun Liu, and Xiaoguang Cheng. Acquisition of data: Yandong Liu, Kai Li, Wenshuang Zhang, Yi Yuan, Kangkang Ma, Fengyun Zhou, Zitong Cheng, Jian Geng, Yongbin Su, and Zhe Guo. Analysis and interpretation of data: Glen M. Blake, Ling Wang, Klaus Engelke, and Annegreet G. Vlug. Drafting of the manuscript: Glen M. Blake, Ling Wang, and Annegreet G. Vlug. Critical revision of the manuscript for important intellectual content: Glen M. Blake, Ling Wang, Annegreet G. Vlug, Klaus Engelke, Yajun Liu, and Xiaoguang Cheng.

ACKNOWLEDGMENTS

The authors thank all participants for their important contributions.

CONFLICT OF INTEREST STATEMENT

Klaus Engelke is a part-time employee of Clario, Inc. The other authors declared no conflict of interest.

ORCID

Xiaoguang Cheng https://orcid.org/0000-0002-4596-8248

REFERENCES

1. Partridge L, Deelen J, Slagboom PE. Facing up to the global challenges of ageing. *Nature*. 2018;561(7721):45-56.
2. Weir CB, Jan A. BMI classification percentile and cut off points. *StatPearls*. StatPearls Publishing; 2023.
3. Oussaada SM, van Galen KA, Cooiman MI, et al. The pathogenesis of obesity. *Metabolism*. 2019;92:26-36.
4. Kuk JL, Saunders TJ, Davidson LE, Ross R. Age-related changes in total and regional fat distribution. *Ageing Res Rev*. 2009;8(4):339-348.
5. Cai Z, He B. Adipose tissue aging: an update on mechanisms and therapeutic strategies. *Metabolism*. 2023;138:155328.
6. Kang PS, Neeland IJ. Body fat distribution, diabetes mellitus, and cardiovascular disease: an update. *Curr Cardiol Rep*. 2023;25(11):1555-1564.
7. Palmer AK, Jensen MD. Metabolic changes in aging humans: current evidence and therapeutic strategies. *J Clin Invest*. 2022;132(16):e158451.
8. Von Bank H, Kirsh C, Simcox J. Aging adipose: depot location dictates age-associated expansion and dysfunction. *Ageing Res Rev*. 2021;67:101259.
9. Borga M, West J, Bell JD, et al. Advanced body composition assessment: from body mass index to body composition profiling. *J Investig Med*. 2018;66(5):1-9.
10. Engelke K, Ghasemikaram M, Chaudry O, et al. The effect of ageing on fat infiltration of thigh and paraspinal muscles in men. *Aging Clin Exp Res*. 2022;34(9):2089-2098.
11. Machann J, Thamer C, Schnoedt B, et al. Age and gender related effects on adipose tissue compartments of subjects with increased risk for type 2 diabetes: a whole body MRI/MRS study. *Magma*. 2005;18(3):128-137.
12. Yu A, Huang M, Wang L, et al. Age and gender differences in vertebral bone marrow adipose tissue and bone mineral density, based on MRI and quantitative CT. *Eur J Radiol*. 2023;159:110669.
13. Guo Z, Blake GM, Li K, et al. Liver fat content measurement with quantitative CT validated against MRI proton density fat fraction: a prospective study of 400 healthy volunteers. *Radiology*. 2020;294(1):89-97.
14. Wang L, Li S, Liu Y, et al. Greater bone marrow fat and myosteatosis are associated with lower vBMD but not asymptomatic vertebral fracture. *Eur Radiol*. 2023;33(1):578-586.
15. Wang L, Yin L, Cheng X, et al. The association of calcium intake with osteoporotic vertebral fractures in a large Chinese cohort. *Aging (Albany NY)*. 2020;12(6):5500-5515.
16. Zhang Y, Zhou Z, Wang C, et al. Reliability of measuring the fat content of the lumbar vertebral marrow and paraspinal muscles using MRI mDIXON-quant sequence. *Diagn Interv Radiol*. 2018;24(5):302-307.
17. Xu Z, Liu Y, Yan C, et al. Measurement of visceral fat and abdominal obesity by single-frequency bioelectrical impedance and CT: a cross-sectional study. *BMJ Open*. 2021;11(10):e048221.
18. Palmer AK, Kirkland JL. Aging and adipose tissue: potential interventions for diabetes and regenerative medicine. *Exp Gerontol*. 2016;86:97-105.
19. Valenzuela PL, Carrera-Bastos P, Castillo-Garcia A, Lieberman DE, Santos-Lozano A, Lucia A. Obesity and the risk of cardiometabolic diseases. *Nat Rev Cardiol*. 2023;20:475-494.
20. Anthony SR, Guarnieri AR, Gozdiff A, Helsley RN, Phillip Owens A, Tranter M. Mechanisms linking adipose tissue inflammation to cardiac hypertrophy and fibrosis. *Clin Sci (Lond)*. 2019;133(22):2329-2344.
21. Lu Z, Tilly MJ, Aribas E, et al. Imaging-based body fat depots and new-onset atrial fibrillation in general population: a prospective cohort study. *BMC Med*. 2022;20(1):317.
22. Chait A, den Hartigh LJ. Adipose tissue distribution, inflammation and its metabolic consequences, including diabetes and cardiovascular disease. *Front Cardiovasc Med*. 2020;7:22.
23. Herrmann M, Engelke K, Ebert R, et al. Interactions between muscle and bone-where physics meets biology. *Biomolecules*. 2020;10(3):432.
24. Veldhuis-Vlug AG, Rosen CJ. Mechanisms of marrow adiposity and its implications for skeletal health. *Metabolism*. 2017;67:106-114.
25. Ecklund K, Vajapeyam S, Feldman HA, et al. Bone marrow changes in adolescent girls with anorexia nervosa. *J Bone Miner Res*. 2010;25(2):298-304.
26. Ali D, Tencerova M, Figeac F, Kassem M, Jafari A. The pathophysiology of osteoporosis in obesity and type 2 diabetes in aging women and men: the mechanisms and roles of increased bone marrow adiposity. *Front Endocrinol (Lausanne)*. 2022;13:981487.
27. Tencerova M, Figeac F, Ditzel N, Taipaleenmaki H, Nielsen TK, Kassem M. High-fat diet-induced obesity promotes expansion of bone marrow adipose tissue and impairs skeletal stem cell functions in mice. *J Bone Miner Res*. 2018;33(6):1154-1165.
28. Attane C, Esteve D, Chaoui K, et al. Human bone marrow is comprised of adipocytes with specific lipid metabolism. *Cell Rep*. 2020;30(4):949-958 e6.
29. Tratwal J, Labella R, Bravenboer N, et al. Reporting guidelines, review of methodological standards, and challenges toward harmonization in bone marrow adiposity research. *Front Endocrinol (Lausanne)*. 2020;11:65.
30. Cheng X, Li K, Zhang Y, et al. The accurate relationship between spine bone density and bone marrow in humans. *Bone*. 2020;134:115312.
31. Wang L, Yin L, Zhao Y, et al. Muscle density discriminates hip fracture better than computed tomography X-ray absorptiometry hip

areal bone mineral density. *J Cachexia Sarcopenia Muscle*. 2020;11(6):1799-1812.
32. Wang L, Yin L, Yang M, et al. Muscle density is an independent risk factor of second hip fracture: a prospective cohort study. *J Cachexia Sarcopenia Muscle*. 2022;13(3):1927-1937.
33. Schwartz AV, Sigurdsson S, Hue TF, et al. Vertebral bone marrow fat associated with lower trabecular BMD and prevalent vertebral fracture in older adults. *J Clin Endocrinol Metab*. 2013;98(6):2294-2300.
34. Woods GN, Ewing SK, Schafer AL, et al. Saturated and unsaturated bone marrow lipids have distinct effects on bone density and fracture risk in older adults. *J Bone Miner Res*. 2022;37(4):700-710.
35. Ma X, Lee P, Chisholm DJ, James DE. Control of adipocyte differentiation in different fat depots; implications for pathophysiology or therapy. *Front Endocrinol (Lausanne)*. 2015;6:1.
36. Bedogni G, Miglioli L, Masutti F, Tiribelli C, Marchesini G, Bellentani S. Prevalence of and risk factors for nonalcoholic fatty liver disease: the Dionysos nutrition and liver study. *Hepatology*. 2005;42(1):44-52.
37. Justesen J, Stenderup K, Ebbesen EN, Mosekilde L, Steiniche T, Kassem M. Adipocyte tissue volume in bone marrow is increased with aging and in patients with osteoporosis. *Biogerontology*. 2001;2(3):165-171.
38. Lifshitz L, Bar Sela S, Gal N, Martin R, Fleitman KM. Iliopsoas the hidden muscle: anatomy, diagnosis, and treatment. *Curr Sports Med Rep*. 2020;19(6):235-243.
39. Ebadi M, Wang CW, Lai JC, et al. Poor performance of psoas muscle index for identification of patients with higher waitlist mortality risk in cirrhosis. *J Cachexia Sarcopenia Muscle*. 2018;9(6):1053-1062.
40. Chaudry O, Grimm A, Friedberger A, et al. Magnetic resonance imaging and bioelectrical impedance analysis to assess visceral and abdominal adipose tissue. *Obesity (Silver Spring)*. 2020;28(2):277-283.

SUPPORTING INFORMATION

Additional supporting information can be found online in the Supporting Information section at the end of this article.

How to cite this article: Wang L, Liu Y, Li K, et al. Age and BMI have different effects on subcutaneous, visceral, liver, bone marrow, and muscle adiposity, as measured by CT and MRI. *Obesity (Silver Spring)*. 2024;32(7):1339-1348. doi:10.1002/oby.24040